

Raman spectroscopy study of graphene thin films synthesized from solid precursor

Jovana Prekodravac¹ · Zoran Marković¹ · Svetlana Jovanović¹ · Ivanka Holclajtner-Antunović² · Vladimir Pavlović³ · Biljana Todorović-Marković¹

Received: 6 November 2015 / Accepted: 9 January 2016 / Published online: 20 January 2016
© Springer Science+Business Media New York 2016

Abstract In this work, we present Raman spectroscopy study of graphene thin films obtained by rapid thermal annealing in vacuum. As a carbon source, we used spectroscopic graphite electrodes cut into small pieces on top of which we deposited copper/nickel thin films. Samples were then annealed at different annealing temperatures (600, 700, 800 and 900 °C) for 30 min. Raman spectroscopy study showed that annealing at lower annealing temperatures (600 and 700 °C) leads to formation of single layer graphene thin films with relatively high level of defects. Annealing at higher annealing temperatures (800 and 900 °C), on the other hand, resulted in formation of homogenous multilayer graphene thin films. From Raman spectra, we also concluded that samples annealed at higher annealing temperatures had lower level of defects compared to the samples annealed at lower annealing temperatures.

Keywords Graphene · Rapid thermal annealing · Raman spectroscopy

1 Introduction

Carbon is one of the most prominent elements on the planet, and thus is quite easy to obtain. The true beauty of graphene is in its simplicity. Graphene is a thick planar sheet with hexagonally arranged carbon atoms. However, as simple as the material is, the

This article is part of the Topical Collection on Advances in the science of light.

Guest Edited by Jelena Radovanovic, Milutin Stepić, Mikhail Sumetsky, Mauro Pereira and Dragan Indjin.

✉ Jovana Prekodravac
prekodravac@vinca.rs; prekodravac@vinca.com

¹ Vinča Institute of Nuclear Sciences, University of Belgrade, Belgrade, Serbia

² Faculty of Physical Chemistry, University of Belgrade, Belgrade, Serbia

³ Joint Laboratory for Advanced Materials, Serbian Academy of Sciences and Arts, Belgrade, Serbia

properties that emerge as a consequence of this simple structure are phenomenal. Because of its structure and properties, it has great potential for application in various fields (Matyba et al. 2010; Yang et al. 2010).

In order to exploit graphene for these applications, several synthesis routes have been employed (Mattevi et al. 2011; Novoselov et al. 2004; Stankovich et al. 2007). However, all of these synthesis routes have their own advantages and limitations.

In this paper, we present graphene synthesis from a solid precursor. As a substrate, and carbon source for graphene synthesis, we used spectroscopic graphite electrodes (99.999 % purity, Ringsdorff Spektralkohlestäbe, höchster Reinheit, SGL Carbon, Germany) cut into small pieces, 1 cm × 1 cm, and polished with diamond pastes. On top of the graphite substrates, we deposited thin copper/nickel (Cu/Ni) films. The deposition was carried out by direct current (DC) sputtering (Balzers Sputtron II system, Switzerland) using 1.3 keV argon (Ar) ions and 99.9 % pure Ni and Cu targets. The base pressure in chamber was 7×10^{-6} mbar and the Ar partial pressure during deposition was 1×10^{-3} mbar. Ni was the first deposited thin metal layer, and Cu was the second one. Thicknesses of individual Ni and Cu films, measured by profilometry, were 50 and 700 nm respectively. Prepared samples were then annealed at different annealing temperatures (600, 700, 800 and 900 °C) for 30 min in a vacuum furnace (TorVac system, United Kingdom) followed by rapid cooling.

Raman spectra of annealed samples were obtained by DXR Raman microscope (Thermo Scientific) using a 532 nm laser as excitation source. The laser power was kept at 2 mW to avoid heating of the sample with a pixel-to-pixel spectral resolution of 1 cm^{-1} . For each sample several Raman spectra were recorded in different positions. The morphology of the films was characterized by scanning electron microscopy (SEM, JEOL JSM-6390LV) in vacuum at room temperature, with 15 kV acceleration voltage. Samples elementary composition was obtained with energy dispersive spectroscopy (EDS, Oxford Aztec X-max). The scanned surface area was $1 \text{ mm} \times 1 \text{ mm}$.

2 Results and discussion

2.1 Raman spectroscopy

Raman spectroscopy is a very important tool for the study of different allotropes of carbon, since it is very sensitive to geometric structure and bonding within molecules (Ferrari and Basko 2013). In graphene Raman spectra the three most prominent bands are the D, G and the 2D bands. The D band appears at around 1350 cm^{-1} and it has been attributed to the in-plane A_{1g} zone edge mode (Dresselhaus et al. 2010). Known also as the defect or the disorder band, D band indicates the level of defects presented in the sample. The G band appears at around 1580 cm^{-1} and corresponds to the in-plane vibration mode involving the sp^2 hybridized carbon atoms that comprise the graphene sheet. The G band position (ω_G) and intensity (I_G) are sensitive to the number of graphene layers (Khan et al. 2014). The most prominent band in graphene Raman spectra is sharp 2D band that appears at around 2700 cm^{-1} . Based on the 2D band intensity (I_{2D}), shape and position (ω_{2D}) it is possible to determine the change in the number of graphene layers presented in the sample (Ferrari et al. 2006; Wu et al. 2014).

Figure 1a presents Raman spectra of the samples annealed for 30 min at different annealing temperatures ranging from 600 to 900 °C. Since the G band position (ω_G) can be

affected by doping, we analyzed the G band intensity (I_G) to determine the change in the number of graphene layers. To do so, all spectra were normalized in respect to the G band intensity. The determined I_G average values were 0.24 ± 0.012 for samples annealed at 600°C , 0.61 ± 0.030 for the sample annealed at 700°C , 1 ± 0.05 for the sample annealed at 800°C and 1.05 ± 0.03 for the sample annealed at 900°C . Therefore, we observed that I_G increases with annealing temperature (Fig. 1b), this change indicates the variation in the number of graphene layers with temperature. From Fig. 1a, it was also noticed that the defect level, determined by the D-to-G band intensity ratio (I_D/I_G), decreases with temperature, which was presented in Fig. 1c. The defect level for samples annealed at 600°C was 0.54 ± 0.027 , for samples annealed at 700°C it was 0.44 ± 0.022 , at 800°C the defect level was determined to be 0.35 ± 0.017 and for samples annealed at 900°C it was 0.33 ± 0.016 . The present defects may originate from graphene edges or from the defects in graphene sheet, but lower values of I_D/I_G suggest the formation of more homogenous and continuous graphene thin films at higher annealing temperatures.

The more precise way to determine the change in the number of graphene layers present in the samples is by analyzing the characteristic of the 2D band. For single layer graphene, 2D band is sharp, symmetric and at least two times higher than the G band (Ferrari 2007; Wu et al. 2014). With rise of the number of graphene layers, the 2D band changes in shape, its intensity (I_{2D}) decreases, while its position shifts to the higher wavenumbers (Ni et al. 2008). In Fig. 2a, we present the change in the 2D band shape, intensity (I_{2D}) and position (ω_{2D}) with the annealing temperature. Here we can see that its shape becomes less symmetric while its intensity (I_{2D}) lowers with increase of annealing temperature. Therefore, in samples annealed at 600 and 700°C , the 2D band is sharp and more than two times intense compared to the G band, which is characteristic for the single layer graphene. In samples annealed at 800 and 900°C , the I_{2D} lowers while its shape becomes less symmetric and shifts to the higher wavenumbers, approximately 20 cm^{-1} . The observed changes at higher annealing temperatures are characteristic for multi layer graphene.

Figure 2b presents change in the number of graphene layers, determined from the 2D-to-G band intensity ratio. Here we can see that the number of graphene layers increases

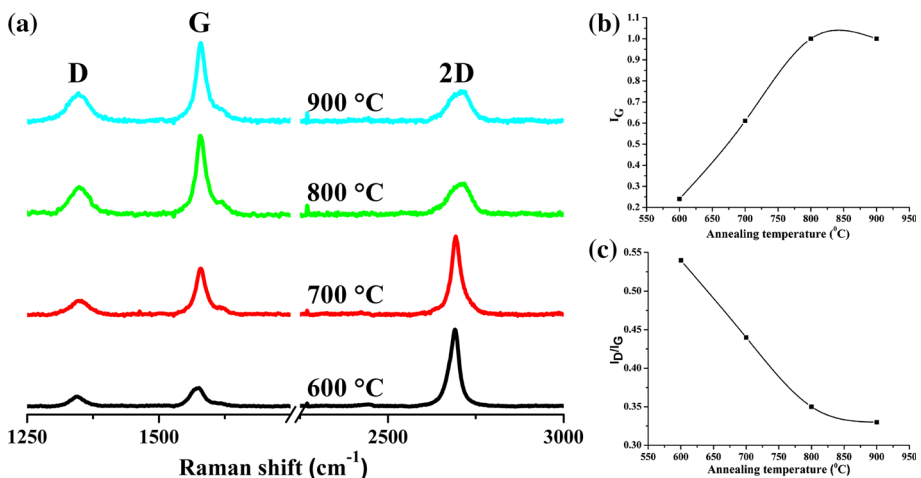


Fig. 1 Raman spectra of formed graphene at different annealing temperatures (a), the G band intensity (b) and the defect level (c) in the function of annealing temperature

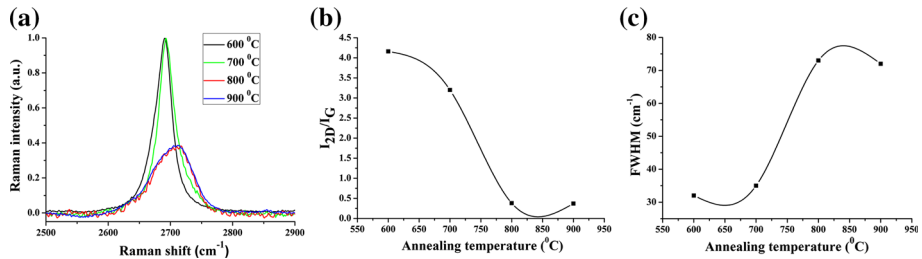


Fig. 2 2D band intensity in the function of annealing temperature (a), 2D-to-G band intensity ratio in the function of temperature (b) and the FWHM values of the 2D band in the function of temperature (c)

Table 1 Data collected from the Raman spectra of the samples annealed at different annealing temperatures

	600 °C	700 °C	800 °C	900 °C
I_G	0.24	0.61	1	1
I_{2D}	1	1	0.38	0.37
ω_{2D} (cm ⁻¹)	2690 ± 0.21	2683 ± 0.18	2716 ± 0.15	2707 ± 0.25
I_D/I_G	0.54	0.44	0.35	0.33
I_{2D}/I_G	4.16	3.20	0.38	0.37
FWHM (2D)	32 ± 0.25 cm ⁻¹	35 ± 0.15 cm ⁻¹	73 ± 0.22 cm ⁻¹	72 ± 0.20 cm ⁻¹

with temperature since the I_{2D}/I_G ratio lowers. The calculated I_{2D}/I_G ratio for samples annealed at different annealing temperatures were 4.15 ± 0.208 at 600 °C, 3.20 ± 0.160 at 700 °C, 0.38 ± 0.019 at 800 °C and 0.37 ± 0.018 at 900 °C. As some authors suggest, the change in the number of graphene layers can be also confirmed with the widening of the 2D band, i.e. by calculating the full width at half maximum (FWHM) of the 2D band (Kim et al. 2012). As it was presented in Fig. 2c, the FWHM values of the 2D band are 32 ± 0.25 cm⁻¹ for samples annealed at 600 °C and 35 ± 0.15 cm⁻¹ for samples annealed at 700 °C, suggesting the formation of single layer graphene. By calculating the FWHM of the 2D band of the sample annealed at 800 °C, we established that it amounts 73 ± 0.22 cm⁻¹, while for the sample annealed at 900 °C it was 72 ± 0.20 cm⁻¹ indicating the formation of multi layer graphene thin films at higher annealing temperatures. All data collected from the Raman spectra presented in Fig. 1a are summarized in Table 1.

In Fig. 3 we present 2D bands from Raman spectra of the samples annealed at 600 and 700 °C fitted with only one Lorentzian curve suggesting the formation of single layer graphene at these temperatures. On the other hand, 2D bands from the Raman spectra of the samples annealed at 800 and 900 °C could not be fitted with less than six Lorentzian curves signifying the formation of multi layer graphene at higher temperatures (Ferrari et al. 2006).

2.2 SEM with EDS probe

Graphene layers synthesized on solid substrate can be imaged using SEM microscopy. The use of SEM also facilitates imaging and EDS analysis of graphene layers with respect to the substrate. In Fig. 4, we present SEM images of the samples annealed at 600 and 900 °C

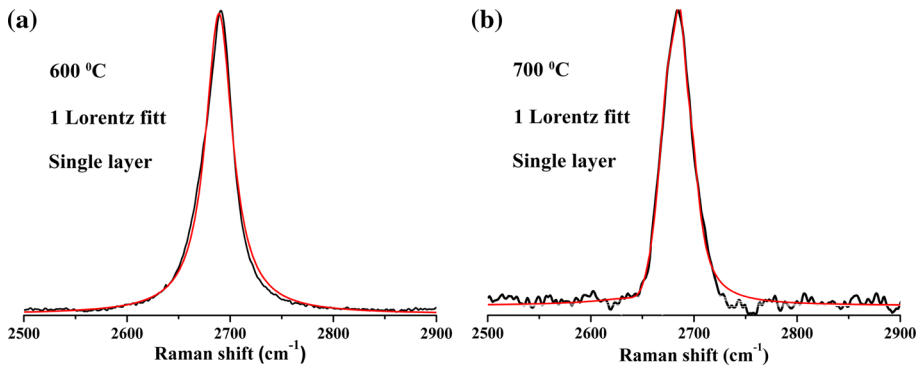


Fig. 3 2D band Lorentz fit from samples annealed at 600 °C (a) and 700 °C (b)

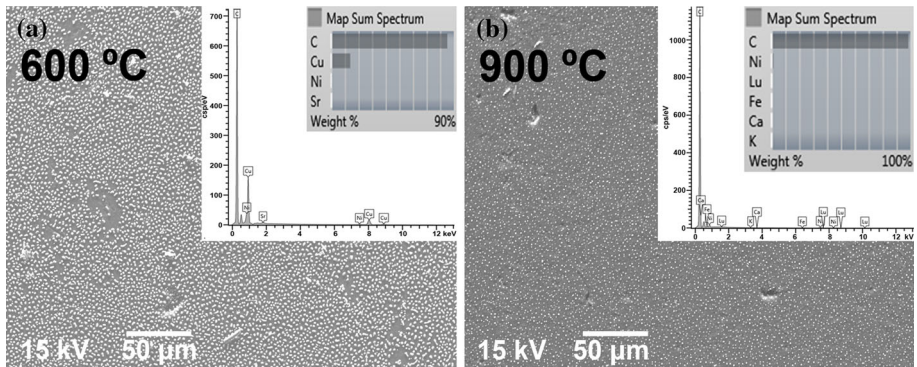


Fig. 4 SEM images of the samples annealed at 600 °C (a) and 900 °C (b) for 30 min and their elemental composition (inset of a and b)

for 30 min. What we can see from Fig. 4a, b is the formation of the Cu/Ni alloy with granular morphology (Subramanian et al. 2005), of approximately 2 μm in size.

Elementary analysis of the sample-scanned area (Fig. 4a inset) confirmed that the most abundant elements on the surface of the sample annealed at 600 °C are carbon with 90 %, Cu with approximately 10 % and Ni in a low percent. In samples annealed at 900 °C, however the most abundant element is carbon with almost 100 % while Ni comes in insignificant percentage, as it is presented in the inset of the Fig. 4b. This clearly indicates the formation of more homogenous and continuous graphene thin films in samples annealed at higher annealing temperatures. This conclusion also explains the lower defect level in these samples.

3 Conclusion

In this paper, we demonstrated that annealing temperature affects graphene synthesis concerning the change in the number of graphene layers. Graphene synthesis at lower annealing temperatures led to the formation of single layer thin films with higher level of

defects. Defects presented in the samples may originate from the fact that at these temperatures there is the formation of Cu/Ni alloy that prevents the formation of continuous graphene films. At higher annealing temperatures, however we observed the formation of multi layer graphene thin films with lower defect level indicating the formation of more homogenous and continuous graphene thin films.

Acknowledgments The Ministry of Education, Science and Technological Development of Republic of Serbia (Project No. 172003) funded this work and bilateral Project Serbia-Slovakia SK-SRB-2013-0044 (451-03-545/2015-09/07).

References

- Dresselhaus, M.S., Jorio, A., Souza, A.G., Saito, R.: Defect characterization in graphene and carbon nanotubes using Raman spectroscopy. *Philos. Trans. R. Soc. A* **368**(1932), 5355–5377 (2010). doi:[10.1098/rsta.2010.0213](https://doi.org/10.1098/rsta.2010.0213)
- Ferrari, A.C.: Raman spectroscopy of graphene and graphite: disorder, electron–phonon coupling, doping and nonadiabatic effects. *Solid State Commun.* **143**(1–2), 47–57 (2007). doi:[10.1016/j.ssc.2007.03.052](https://doi.org/10.1016/j.ssc.2007.03.052)
- Ferrari, A.C., Basko, D.M.: Raman spectroscopy as a versatile tool for studying the properties of graphene. *Nat. Nanotechnol.* **8**(4), 235–246 (2013). doi:[10.1038/nnano.2013.46](https://doi.org/10.1038/nnano.2013.46)
- Ferrari, A.C., Meyer, J.C., Scardaci, V., Casiraghi, C., Lazzeri, M., Mauri, F., Piscanec, S., Jiang, D., Novoselov, K.S., Roth, S., Geim, A.K.: Raman spectrum of graphene and graphene layers. *Phys. Rev. Lett.* (2006). doi:[10.1103/Physrevlett.97.187401](https://doi.org/10.1103/Physrevlett.97.187401)
- Khan, M.F., Iqbal, M.Z., Iqbal, M.W., Eom, J.: Improving the electrical properties of graphene layers by chemical doping. *Sci. Technol. Adv. Mater.* (2014). doi:[10.1088/1468-6996/15/5/055004](https://doi.org/10.1088/1468-6996/15/5/055004)
- Kim, K., Coh, S., Tan, L.Z., Regan, W., Yuk, J.M., Chatterjee, E., Crommie, M.F., Cohen, M.L., Louie, S.G., Zettl, A.: Raman spectroscopy study of rotated double-layer graphene: misorientation-angle dependence of electronic structure. *Phys. Rev. Lett.* (2012). doi:[10.1103/Physrevlett.108.246103](https://doi.org/10.1103/Physrevlett.108.246103)
- Mattevi, C., Kim, H., Chhowalla, M.: A review of chemical vapour deposition of graphene on copper. *J. Mater. Chem.* **21**(10), 3324–3334 (2011). doi:[10.1039/c0jm02126a](https://doi.org/10.1039/c0jm02126a)
- Matyba, P., Yamaguchi, H., Eda, G., Chhowalla, M., Edman, L., Robinson, N.D.: Graphene and mobile ions: the key to all-plastic, solution-processed light-emitting devices. *ACS Nano* **4**(2), 637–642 (2010). doi:[10.1021/nn9018569](https://doi.org/10.1021/nn9018569)
- Ni, Z.H., Wang, Y.Y., Yu, T., Shen, Z.X.: Raman spectroscopy and imaging of graphene. *Nano Res* **1**(4), 273–291 (2008). doi:[10.1007/s12274-008-8036-1](https://doi.org/10.1007/s12274-008-8036-1)
- Novoselov, K.S., Geim, A.K., Morozov, S.V., Jiang, D., Zhang, Y., Dubonos, S.V., Grigorieva, I.V., Firsov, A.A.: Electric field effect in atomically thin carbon films. *Science* **306**(5696), 666–669 (2004). doi:[10.1126/science.1102896](https://doi.org/10.1126/science.1102896)
- Stankovich, S., Dikin, D.A., Piner, R.D., Kohlhaas, K.A., Kleinhammes, A., Jia, Y., Wu, Y., Nguyen, S.T., Ruoff, R.S.: Synthesis of graphene-based nanosheets via chemical reduction of exfoliated graphite oxide. *Carbon* **45**(7), 1558–1565 (2007). doi:[10.1016/j.carbon.2007.02.034](https://doi.org/10.1016/j.carbon.2007.02.034)
- Subramanian, B., Jayakumar, S., Jayachandran, M., Jayakrishnan, S.: Studies on nickel electrodeposits on dc magnetron sputtered copper substrates. *Surf. Eng.* **21**(2), 151–155 (2005). doi:[10.1179/174329405x40858](https://doi.org/10.1179/174329405x40858)
- Wu, J.B., Zhang, X., Ijas, M., Han, W.P., Qiao, X.F., Li, X.L., Jiang, D.S., Ferrari, A.C., Tan, P.H.: Resonant Raman spectroscopy of twisted multilayer graphene. *Nat. Commun.* **5**, 5309 (2014). doi:[10.1038/ncomms6309](https://doi.org/10.1038/ncomms6309)
- Yang, K., Zhang, S.A., Zhang, G.X., Sun, X.M., Lee, S.T., Liu, Z.A.: Graphene in mice: ultrahigh in vivo tumor uptake and efficient photothermal therapy. *Nano Lett.* **10**(9), 3318–3323 (2010). doi:[10.1021/NL100996u](https://doi.org/10.1021/NL100996u)